Published in final edited form as:

Curr Biol. 2018 April 02; 28(7): 1124–1131.e3. doi:10.1016/j.cub.2018.02.039.

MAMMALIAN OOCYTES LOCALLY REMODEL FOLLICULAR ARCHITECTURE TO PROVIDE THE FOUNDATION FOR GERM LINE-SOMA COMMUNICATION

Stephany El-Hayek[1,2,4], **Qin Yang**[4], **Laleh Abbassi**[1,3,4], **Greg FitzHarris**[5], and **Hugh J. Clarke**[1,2,3,4]

[1]Department of Obstetrics and Gynecology, McGill University, Montreal, Canada H4A 3J1

[2]Department of Biology, McGill University, Montreal, Canada H4A 3J1

[3]Division of Experimental Medicine, McGill University, Montreal, Canada H4A 3J1

[4]Research Institute – McGill University Health Centre, 1001 Boul. Décarie, Montreal, Canada H4A 3J1

[5]Centre Recherche CHUM and Département d'Obstétrique et de Gynécologie, Université de Montréal, 900 rue St-Denis, Montreal, Canada H2X 0A9

eTOC blurb

El-Hayek et al. show that the growing oocyte induces the somatic cells surrounding it to continuously generate specialized filopodia which penetrate its extracellular coat and permit essential germ line-somatic communication. Fewer filopodia couple the two cell types in aged females, impairing communication and suggesting a basis for infertility.

Lead contact and Corresponding Author: Hugh Clarke, Room E-M0.3211, McGill University Health Centre, 1001 Boul. Decarie, Montreal, CANADA H4A 3J1, Hugh.clarke@mcgill.ca.

DECLARATION OF INTERESTS

The authors declare no competing interests

AUTHOR CONTRIBUTIONS

Conceptualization, S.E.H. and H.J.C.; Methodology, S.E.H. and H.J.C.; Investigation, S.E.H., Q.Y. and L.A.; Resources, H.J.C. and G.F.; Writing – Original Draft, H.J.C. and S.E.H.; Writing – Review & Editing, H.J.C., S.E.H. and G.F.; Funding Acquisition, H.J.C. and G.F.; Supervision, H.J.C.

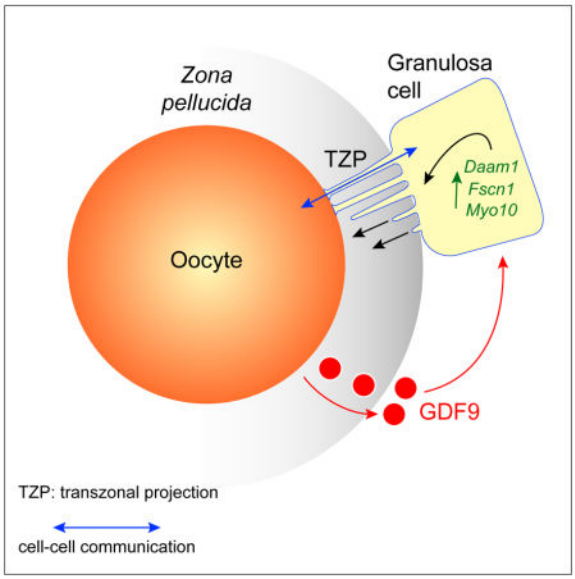

Keywords

oocyte; follicle; intercellular signalling; filopodia; fertility

SUMMARY

Germ cells develop in a microenvironment created by the somatic cells of the gonad [1–3]. Although in males the germ and somatic support cells lie in direct contact, in females a thick extracellular coat surrounds the oocyte, physically separating it from the somatic follicle cells [4]. To bypass this barrier to communication, narrow cytoplasmic extensions of the follicle cells traverse the extracellular coat to reach the oocyte plasma membrane [5–9]. These delicate structures provide the sole platform for the contact-mediated communication between the oocyte and its follicular environment that is indispensable for production of a fertilizable egg [8, 10–15]. Identifying the mechanisms underlying their formation should uncover conserved regulators of fertility. We show here in mice that these structures, termed transzonal projections (TZPs), are specialized filopodia whose number amplifies enormously as oocytes grow, enabling increased germ-soma communication. By creating chimeric complexes of genetically tagged oocytes and follicle cells, we demonstrate that follicle cells elaborate new TZPs that push through the extracellular coat to reach the oocyte surface. We further show that growth-differentiation factor 9 produced by the oocyte drives the formation of new TZPs, uncovering a key yet unanticipated role for the germ cell in building these essential bridges of communication. Moreover, TZP-number and germline-soma communication are strikingly reduced in reproductively aged females. Thus, the growing oocyte locally remodels follicular architecture to ensure that its developmental needs are met, and an inability of somatic follicle cells to respond appropriately to oocyte-derived cues may contribute to human infertility.

RESULTS AND DISCUSSION

TZPs are specialized filopodia

Prior to ovulation and fertilization, mammalian oocytes undergo a prolonged period of growth within the ovarian follicle [16]. During this phase, which lasts 3–4 months in humans, the oocyte increases >100-fold in volume as it accumulates messenger RNAs, protein and organelles that will direct early embryonic development. Concomitant with oocyte growth, the adjacent follicular granulosa cells proliferate so that they continue to fully cover its expanding surface area. In primordial follicles housing non-growing oocytes, the two cell types lie directly apposed. Shortly after entry into the growth phase, however, the extracellular coat, termed the *zona pellucida* in mammals, becomes assembled [4]. Although the deposition and progressive thickening of the *zona pellucida* coat displaces the bodies of the granulosa cells away from the oocyte, TZPs traverse it to reach the oocyte surface [5–9, 17, 18] (Figure 1A). Most TZPs contain a central core of actin [6, 8, 9] (Figure 1B), whereas a much smaller number contain tubulin [8, 17] (Figure 1C). Multiple TZPs typically project from each granulosa cell adjacent to the *zona pellucida*, sometimes appearing to extend from a single point of origin (Figure 1B, middle; see also Figure 2F). Long actin-rich filaments also project from some granulosa cells located in more distal layers and appear to reach the oocyte (Figure 1B, right, arrows).

Because TZPs morphologically resemble filopodia, which range from 0.1–0.4 μm in diameter and 1–200 μm in length and also contain an actin core [19], we examined whether they shared structural elements. We detected both DAAM1 (dishevelled-associated activator of morphogenesis 1), a formin family member that controls nucleation and elongation of new actin filaments [20], and fascin, which bundles and strengthens the parallel actin filaments in filopodia [21], along the axis of the TZPs (Figure 1D, E). MYO10, which promotes filopodial growth [22], was present in large foci at the apical (oocyte-facing) membrane of granulosa cells in the innermost layer immediately adjacent to the oocyte (Figure 1F). These results indicate that TZPs are specialized filopodia that project from the granulosa cells to the growing oocyte.

Granulosa cells elaborate new TZPs during oocyte growth

To determine how TZPs are generated, we first quantified the number of TZPs at different stages of growth. We observed a striking increase in the number of actin-TZPs as oocytes increased in size (Figure 2A). We observed the same robust increase using a fluorescent dye, FM1-43, to label the plasma membrane of the TZPs (Figure S1A). In contrast, tubulin-TZPs were almost two orders of magnitude less abundant than the actin-rich TZPs and did not detectably increase in number during oocyte growth (Figure 2B). When we incubated granulosa cell-oocyte complexes (GOCs) under conditions that support oocyte growth, we observed a 2.5-fold increase in the number of actin-TZPs per equatorial section over a 5-day culture period (Figure 2C). Since oocyte diameter increased by 1.1-fold, the TZP density also increased during the culture. Thus, as oocytes grow and their surface area expands, there is a continuous increase in the number and density of TZPs.

Oocyte growth is accompanied by proliferation of the surrounding granulosa cells, ensuring that they fully cover the expanding surface of the oocyte. We hypothesized that the newly produced granulosa cells elaborate new TZPs, thereby generating the observed increase in TZP-number (Figure S1B). To test this idea, we used transgenic mTmG mice expressing membrane-targeted Tomato, a modified form of red fluorescent protein (RFP) that can be detected using anti-RFP antibodies [23], in a cell-reaggregation assay. Anti-RFP stains the cell bodies and TZPs of the granulosa cells and the oocyte membrane of mTmG mice but not of wild-type mice (Figure 2D). This allowed us to unambiguously identify the genotype of individual cells. We collected GOCs containing mid-growth stage oocytes fully enclosed by a *zona pellucida* from wild-type and mTmG mice, disaggregated the cells, and then combined oocytes of each genotype with a mixture of wild-type and mTmG granulosa cells to create chimeric complexes (Figure 2E, left). After a 5-day incubation, we recovered the reaggregated complexes and examined them using confocal microscopy to determine whether TZPs were present. Crucially, because a *zona pellucida* enclosed the oocytes when the complexes were constructed, any labelled TZPs that projected to an unlabelled oocyte (or vice-versa) could only have been produced by *de novo* generation and penetration through the *zona pellucida*.

The complexes that we recovered morphologically resembled intact GOCs (Figure 2E, right). Actin-rich filaments extended from the granulosa cells to the oocyte; crucially, these included filaments extending from mTmG granulosa cells to wild-type oocytes (Figure 2F, upper). When we improved optical resolution by removing the bodies of the granulosa cells, we observed an enlarged area of staining where the Tomato-labelled filaments contacted the oocyte surface (Figure 2F, middle, asterisks). These strikingly resemble the bulbous swellings observed at the tips of TZPs (Figure 1A, right) [9, 17]. Conversely, we also observed non-labelled actin-rich filaments extending from non-labelled (wild-type) granulosa cells to mTmG oocytes (Figure 2F, lower). We also observed filaments containing tubulin (Figure 2G) but, as in intact complexes, these were rare. These results demonstrated that granulosa cells elaborate filaments that penetrate through the *zona pellucida* to reach the oocyte surface.

To test whether these filaments were genuine TZPs, we examined gap junctional communication between the oocyte and granulosa cells, as this is an essential function of TZPs [8]. By thirty minutes after injection of a gap junction-permeable fluorescent dye into the oocyte of reaggregated complexes, fluorescence was easily detected in the surrounding granulosa cells (Figure 2H, upper). The granulosa cell fluorescence was completely abolished, however, when we incubated the reaggregates in a pharmacological inhibitor of gap junction activity prior to injection (Figure 2H, lower). Thus, functional gap junctions were assembled where the newly generated filaments contacted the oocyte membrane. These results direct prove that granulosa cells elaborate new TZPs that penetrate through the *zona pellucida* to the oocyte surface. We conclude that the enormous increase in the number of TZPs during oocyte growth is largely driven by the generation of new TZPs by the granulosa cells.

GDF9 produced by the oocyte promotes generation of TZPs by granulosa cells

We next asked how the generation of TZPs is regulated. Oocyte and follicular development depend crucially on bi-directional communication between the germ-line and somatic compartments [15, 24, 25]. On one hand, the granulosa cells send signals that trigger oocytes in primordial follicles to initiate growth, provide essential metabolites to growing oocytes, and regulate entry of fully grown oocytes into meiotic maturation [10, 16, 26, 27]. On the other hand, oocytes produce factors that promote proliferation and differentiation of the granulosa cells [15, 24, 25]. This germ line-somatic regulatory loop ensures the development of a fertilizable egg. Growth-differentiation factor (GDF) 9, a TGFβ-type growth factor produced by oocytes, exerts multiple effects on granulosa cell physiology [24, 25, 28]. Intriguingly, the TZPs of mice lacking GDF9 are morphologically abnormal and their oocytes fail to develop normally [29, 30]. Moreover, the SMAD signaling pathway, which transduces TGFβ signals, regulates *Myo10* and *Fscn1* levels in somatic cells [31]. These observations suggested that oocyte-derived GDF9 might generate or maintain TZPs.

To test this idea, we first used a technique termed oocytectomy to remove the oocyte from cumulus granulosa cell-oocyte complexes [32] (Figure 3A, left), thereby eliminating the source of oocyte-derived factors including GDF9. Following incubation of the remaining shell of granulosa cells, the quantities of *Daam1*, *Fscn1* and *Myo10* mRNAs were reduced by about 70% (Figure 3A, right). Strikingly, this loss was fully or partially rescued by adding recombinant mouse GDF9 [28] to the culture medium. Next, we turned to GOCs, in which new TZPs are being steadily generated. Incubation of GOCs for 5 days in the presence of GDF9 increased the amount of all three mRNAs in the granulosa cells (Figure 3B), as well as the number and density of TZPs (Figure 3C). In contrast, incubation of complexes in the presence of an inhibitor of the SMAD2/3 pathway led to a reduction both in the amounts of the three mRNAs (range: ~25% to ~75%) in the granulosa cells and in the number of TZPs (~70%) (Figures 3D, 3E). These results established that GDF9 via SMAD signaling can promote the generation of TZPs.

To directly test whether oocyte-derived GDF9 generates TZPs, we injected short interfering (si) RNA targeting *Gdf9* or a control into oocytes within GOCs. The injected siRNA reduced oocyte *Gdf9* RNA by ~70% and GDF9 protein by ~60% (Figure 3F), whereas other proteins remained unchanged (Figure S2). The surrounding granulosa cells contained less phosphorylated SMAD2/3 (Figure 3G), altogether establishing that GDF9 signalling was reduced. In GOCs incubated for five days after RNAi injection, we observed a ~50% decrease in the quantities of *Fscn1* and *Myo10* mRNAs in the granulosa cells (Figure 3H). *Daam1* mRNA did not detectably decline when oocyte GDF9 was depleted, in contrast to the decline observed following oocyte removal, suggesting that other oocyte-secreted factors may contribute to regulating its expression. Crucially, we observed that the number of TZPs was reduced to 30% of that of injected controls (Figure 3H). Moreover, adding GDF9 to the culture medium following siRNA injection restored the number of TZPs to 60% of the controls. These results establish that GDF9 produced by the oocyte induces neighbouring granulosa cells to increase the steady-state levels of mRNAs encoding structural components of TZPs and to generate new TZPs.

TZP number and function are reduced in reproductively aged females

Oocyte quality declines as females age [33]. Although multiple defects have been identified in these oocytes [34–37], when and how during oocyte development they arise is not known. In view of the crucial role of communication between the oocyte and its follicular microenvironment, we speculated that a reduction in the number of TZPs might be associated with ageing. We observed that the number of TZPs was reduced by 40% in the aged females (Figure 4A), even though their oocytes reached full size, as previously reported [38]. Using a confocal imaging-based technique known as fluorescence loss in photobleaching [39], we then tested whether the reduced number of TZPs was associated with impaired gap junctional communication. Briefly, after loading a gap junction-permeable fluorescent dye into GOCs, a laser is used to bleach the fluorescence in the oocyte. The loss of fluorescence in the neighbouring granulosa cells quantitatively measures the degree of gap junctional coupling between the two cell types. We observed significantly slower loss of fluorescence in the granulosa cells of complexes of aged females as compared with young females (Figure 4B), indicating that there is less gap junctional coupling between the oocyte and granulosa cells.

Strikingly, *Daam1*, *Fscn1*, and *Myo10* mRNAs also were reduced by 60–70% in the granulosa cells of aged females (Figure 4C). In contrast, we found no difference in the amount of *Gdf9* mRNA or GDF9 protein in their oocytes (Figure S3), consistent with previous studies [40]. These results suggest that the capacity of granulosa cells to elaborate TZPs in response to oocyte-derived signals might become impaired with age. It is also possible that oocyte-derived signals other than GDF9 weaken with age or that the TZPs of aged granulosa cells are relatively unstable. In any case, these results identify impaired communication between the oocyte and its follicular environment as a novel defect associated with reproductive ageing.

CONCLUSION

We show here that TZPs are specialized filopodia that are actively and continuously generated during the growth phase of oogenesis and identify a key role for the oocyte itself, via secreted GDF9, in inducing their formation. These findings differ sharply from the long-standing view that TZPs arise passively as the thickening of the *zona pellucida* pushes the granulosa cells away from the oocyte [41]. Our findings are, however, consistent with and provide a simple mechanistic basis for previous observations that gap junctional coupling between these two cell types increases during oocyte growth [39, 42]. When this coupling is genetically abrogated, oocytes arrest growth before they reach full size and cannot give rise to embryos [2, 12]. Thus, the growing oocyte directs local remodeling of the follicular architecture to ensure that its developmental needs are met.

Our observation that GDF9 increases the amounts of mRNAs encoding key structural components of filopodia suggests a mechanism for this follicular remodelling. We suggest that the increased mRNAs promote the generation of new TZPs, enabling more efficient transfer of metabolites from the granulosa cells to the oocyte. This stimulates increased GDF9 production by the oocyte, promoting the formation of more TZPs and further enhancing granulosa cell-oocyte communication and exchange. Other oocyte-secreted

factors may also promote formation of TZPs, independently or co-operatively with GDF9. This model identifies a mechanism by which signaling through the germ line-soma regulatory loop [15] may become amplified during oocyte growth and differentiation.

Why do TZPs grow towards the oocyte? The accumulation of MYO10 near the *zona pellucida*-adjacent membrane of the inner granulosa cells suggests that they are polarized, possibly by interaction with the z*ona pellucida* or by diffusible factors secreted by the oocyte. In this context, we note that the TZP-like filaments that extend from granulosa cells of distal layers towards the oocyte could have been generated while these cells were adjacent to the *zona pellucida*, after which the cells became displaced to outer layers. The close packing of the granulosa cells may also restrict TZP growth to the free surface facing the oocyte. Once TZPs reach the oocyte surface, they likely establish a stable interaction, as indicated by the presence of *zonula adherens* [9] and desmosome-like junctions [43] at the points of contact.

By providing evidence that defective germ line-soma communication may underpin the age-associated decline in oocyte quality, our results have important implications for understanding infertility in women. Although the loss of oocyte quality is often considered to originate within the germ cell, granulosa cells of aged individuals also are defective [44, 45]. Our results identify a specific defect in germ-line soma interaction in aged females and link this to reduced expression of relevant genes in the granulosa cells. While this reduction could be due to impaired signaling from the oocyte, it may indicate that the primary lesion underlying poor oocyte quality originates in the somatic compartment of the follicle. In this light, it is striking that certain disease conditions that are associated with poor oocyte quality are marked by reduced gap junctional coupling between the oocyte and granulosa cells [46]. These observations raise the intriguing possibility that a common etiological origin may underlie the decline in oocyte quality associated with a diverse range of natural and pathological infertilities.

STAR METHODS

CONTACT FOR REAGENT AND RESOURCE SHARING

Further information and requests for resources and reagents should be directed to and will be fulfilled by the Lead Contact, Hugh Clarke (hugh.clarke@mcgill.ca).

EXPERIMENTAL MODEL AND SUBJECT DETAILS

Mice—All experiments were performed in compliance with the regulations and policies of the Canadian Council on Animal Care and were approved by the Animal Care Committee of the Research Institute of the McGill University Health Centre (RI-MUHC). CD-1 mice were obtained from Charles River (St-Constant, QC). mTmG (membrane-Tomato/membrane-Green) founder mice were obtained (Jackson Laboratory, Bar Harbor, ME; strain 007676) and a colony established at the RI-MUHC. These mice possess cassette encoding a membrane-targeted tdTomato. Targeting is mediated by fusion of the first 8 amino acids of the plasma membrane-associated protein, MARCKS, to the N-terminal of tdTomato.

METHOD DETAILS

Collection and culture of cells—Granulosa cell-oocyte complexes (GOCs), cumulus-oocyte complexes (COCs) and denuded oocytes were obtained as previously described [39, 47]. Briefly, ovaries were removed from the mice and the cell complexes were recovered and collected in HEPES-buffered minimal essential medium (MEM, pH 7.2, Life Technologies, Burlington, ON), then cultured in $NaHCO_3$-buffered MEM in an atmosphere of 5% CO_2 in air. GOCs were obtained by incubating ovaries of 10- to 12-day old mice in the presence of collagenase (10 μg/ml; Cedarlane, Burlington, ON) and DNase I (10 μg/ml; Sigma) at 37°C in air. At 2- to 3-minute intervals, the fragments were gently pipetted to disrupt them. Individual GOCs were collected using a mouth-controlled micropipette and transferred to fresh medium. COCs were obtained by puncturing ovaries of 19- to 21-day old mice, which had received an intraperitoneal injection of 5 IU of equine chorionic gonadotropin 44 hr previously, using 30G1/2 needles. The COCs were collected using a mouth-controlled micropipette and transferred to a fresh dish of medium. Denuded oocytes were obtained by removing the granulosa or cumulus cells using a fine-bore mouth-controlled micropipette. GOCs were used in most experiments, as these are at a stage where TZP-number is steadily increasing and continue to grow when maintained in vitro. COCs were used for experiments in which the oocyte was removed from the complex and when comparing young and aged mice, as oocytectomy of GOCs is technically difficult and GOCs are difficult to recover from aged mice.

To grow oocytes *in vitro*, GOCs were transferred to type I collagen 3.0-micron inserts (Becton-Dickinson, Mississauga, ON) in 24-well plates containing 750 μl of MEM supplemented with ITS (Sigma), cilostamide (10 μM, Sigma), and FSH (10 mIU/ml; EMD Serono, Mississauga, ON), in a modification of the original method [47]. Two-thirds of the medium was replaced every third day. Where appropriate, mouse growth-differentiation factor 9 (GDF9, 100 ng/mL, R&D Systems, Minneapolis, MN) or SB431542 (10 μM, Sigma) was added to the medium. To remove the oocyte from COCs (oocytectomy), these were punctured using a fine glass needle.

Construction of and analysis of granulosa cell-oocyte reaggregates—Modifying a published procedure [48], GOCs obtained from 12-day mice were incubated in Ca-Mg-free PBS and drawn in and out of a mouth-controlled micropipette to generate a suspension of denuded oocytes surrounded by the *zona pellucida* and individual or small clumps of granulosa cells. Twenty-five oocytes and disaggregated granulosa cells were deposited into the base of a 200-μl microfuge tube and PBS was added to a total volume of 100 μl. The tube was spun at top speed in a microcentrifuge for one minute, then rotated 180° and centrifuged for one minute. This step was repeated twice more. The tube was then cut near the base and the cell-pellet was carefully scooped out and incubated for 6 days in a tissue-culture dish in α-MEM supplemented with 10 IU/mL FSH, 10 nM estradiol and 100 ng/mL GDF9. Half of the medium was changed after three days. Following incubation, the mass of cells was gently teased apart and granulosa cell-oocyte aggregates that resembled GOCs, were individually isolated. For TZP analysis, these were fixed and stained either as intact complexes or after removal of some of the granulosa cells to improve visualization of the TZPs. Anti-RFP was used to detect Tomato, as the endogenous fluorescence could not be

detected when complexes or intact GOCs were imaged in the equatorial plane. For Lucifer Yellow injections, the oocyte of each complex was injected with about 10 pl of a 100 mM solution of Lucifer Yellow (Thermo Fisher). The complexes were incubated for 30 minutes, then examined using a fluorescence microscope. To block gap junctional transmission, some complexes were incubated in carbenoxolone for 30 minutes prior to, as well as following, injection.

Image analysis—To visualize TZPs in living oocytes, they were freed of the granulosa or cumulus cells by physical disruption, immediately washed in ice-cold PBS, then incubated in FM 1–43 (5 μg/ml, Life Technologies) in ice-cold PBS for 15 minutes. Oocytes were imaged while still in the staining solution in Fluorodish cell culture dishes (World Precision Instruments, Sarasota, FL). For analyses of fixed cells, GOCs, COCs or oocytes were fixed for 15 min at room temperature (RT) in freshly prepared 2% *para*-formaldehyde in phosphate-buffered saline (PBS), then washed with PBS containing Tween-20 (PBST, 0.1%, Sigma). To stain actin, cells were incubated for 1 hr at RT in fluorochrome-conjugated phalloidin diluted 1:100 in PBST. For immunofluorescence, cells were fixed as above, except those used to detect fascin, which were fixed in methanol for 5 min at -20°C. Fixed cells were permeabilized in PBST, then incubated overnight in the primary antibody in PBST at 4°C with gentle agitation, washed twice in PBST, then incubated for 1 hr at RT in the secondary antibody in PBST. To mount the cells, a 9 mm × 0.12 mm spacer (GBL654008, Sigma) was attached to a glass microscope slide. A 2-μl drop of PBS was placed in the centre of the spacer and covered with 20 μl of mineral oil. Cells were then transferred into the drop of PBS and a cover slip was placed on top. Images were acquired using Zeiss LSM 510 and LSM 880 confocal microscopes (Zeiss, Toronto, ON).

To measure the diameter of oocytes within the complexes, pseudo-brightfield images at the maximum diameter were acquired using the confocal microscope and analyzed using the software provided by the manufacturer. To quantify the number of actin, tubulin, or total TZPs, images were analyzed using Image J (National Institutes of Health, Bethesda, MD) in a confocal optical section obtained at the equatorial plane of the oocyte. Using four 10-μm arcs set 90° apart around the oocyte circumference, we counted the number of peaks of fluorescence above a threshold set at 20% of the intensity of the oocyte cortex. The average number of peaks per arc was then calculated and using the oocyte diameter this was converted this to an estimate of the total number of TZPs in the equatorial plane.

For immunohistochemistry, ovaries were fixed and processed as described [39]. Sections were cut at 5 μm, deparaffinized and rehydrated, then boiled for 40 min in Tris-EDTA (pH 9.0). After cooling to RT, slides were blocked with 1.35% goat serum in PBST for 30 min at RT in a humidified chamber. Following PBST washes, slides were incubated at 4°C overnight in anti-MYO10 (Sigma), then washed in PBST and incubated for 1 hr at RT in anti-rabbit Alexa 488. Then were then washed and mounted using Mowiol (Sigma) and examined using the CLSM 510 microscope.

Samples for electron microscopy were fixed in 2.5% glutaraldehyde in 0.1M sodium cacodylate buffer (all reagents from Electron Microscopy Sciences, except as indicated) overnight at 4°C, then washed and post-fixed in 1% osmium and 1.5% potassium

ferrocyanide. Following dehydration to acetone (ThermoFisher), they were infiltrated with increasing concentrations of Epon and embedded in 100% Epon for 48 hr at 60°C. Sections of 100 nm thickness were cut using a Leica ECT microtome, placed onto a 200-mesh formar-coated copper grid and post-stained using 4% uranyl acetate and Reynold's lead. Images were obtained and recorded using a FEI Tecnai 12 BioTwin TEM equipped with an AMT XR80C CCD camera at an accelerating voltage of 120 kV.

RNA purification and quantitative real-time PCR—RNA was extracted using a Picopure RNA isolation kit (Life Technologies) following the manufacturer's instructions and eluted in 10 μl of the provided elution buffer, as described [39]. Briefly, SuperScript II Reverse Transcription kit (Life Technologies) was used to generate cDNA. PCR amplification was performed using a Corbett Rotorgene 6000 (Montréal Biotech, Montreal, QC). Each reaction contained 4 μl of EvaGreen Mix (Montréal Biotech), 13 μl of UltraPure DNase/RNase-free distilled water (Life Technologies), 1 μl of 10 μM primers and 2 μl of cDNA (diluted by 1:20 from original stock). Primers were designed using Primer-BLAST (National Institutes of Health) and obtained from Sigma. Primer sequences are given in Key Resources Table. For each primer pair, a standard curve was generated using serial dilutions of cDNA prepared from ovarian RNA and used to determine the efficiency of amplification. Melt-curve analysis and electrophoresis of amplified products confirmed that only a single product of the expected size was generated. Data was analyzed using software provided by the manufacturer. Relative quantities of amplified product were calculated according to $2^{-\Delta\Delta CT}$ method, using *Actb* for normalization.

Microinjection of siRNA—GOCs were collected from 12- to 14-day old mice. Using a Zeiss Axio Observer Z1 microscope and PLI-100 microinjector (Medical Systems, NY), approximately 10 pl of a 20 μM solution of siRNA (GE Dharmacon) targeting either *Gdf9* (GGUUUUAUGUGACGGAAGA) or *Rspo1* as a control (CUGUUCAGAAGUCAACGGUU) was injected into the oocyte. Following injection, GOCs were transferred to MEM supplemented with ITS and FSH as above and incubated for up to 5 days. All data was generated using at least three independent biological replicates.

Analysis of gap junctional coupling using fluorescence loss in photobleaching (FLIP)—FLIP was performed as previously described [39]. GOCs were incubated for 15 min in MEM containing freshly prepared calcein-AM (Thermo Fisher) and then transferred in to calcein-free MEM for 60 min to allow dye transfer into the oocyte. Sixty bleaches of 50 iterations over a period of one minute were then performed using the argon laser at 50% transmission strength on a circular area of 10-μm diameter at the center of the oocyte. At every 10th time-point, the intensity of fluorescence in the oocyte and the layer of granulosa cells immediately surrounding it was recorded before and after bleaching. Loss of fluorescence was then calculated as described [39].

QUANTIFICATION AND STATISTICAL ANALYSIS

Statistical analysis was performed using GraphPad Prism 6.0. Single-sample *t*-test, two-sample *t*-test, or one-way ANOVA followed by Tukey HSD test was used, depending on the

experiment. Reported values are the mean ± standard error of the mean of three or more independent biological experiments. $p<0.05$ was considered significant, and is indicated by asterisks for *t*-test or different letters above the histogram bars for ANOVA.

Supplementary Material

Refer to Web version on PubMed Central for supplementary material.

Acknowledgments

Supported by grants from the Eunice Kennedy Shriver National Institute of Child Health & Human Development of the National Institutes of Health (R21HD086407), Canadian Institutes of Health Research (CIHR), the Natural Sciences and Engineering Research Council of Canada, and the Research Institute of the McGill University Health Centre (RI-MUHC) to H.J.C. and from the CIHR to G.F. S.E.H. was supported by the CIHR Training Program in Reproduction, Early Development, and the Impact on Health; the Réseau Québécois en Reproduction; and the RI-MUHC. We deeply thank Shoma Nakagawa for invaluable assistance performing experiments, Jeannie Mu (Facility for Electron Microscopy Research of McGill University) and Min Fu (RI-MUHC Imaging Platform) for technical support, and Marie-Émilie Terret (Collège de France) for suggestions on the manuscript. We apologize to colleagues whose work could not be cited owing to editorial policies. Research reported in this publication is solely the responsibility of the authors and does not necessarily represent the official views of the National Institutes of Health.

References

1. Matunis EL, Stine RR, de Cuevas M. Recent advances in Drosophila male germline stem cell biology. Spermatogenesis. 2012; 2:137–144. [PubMed: 23087833]
2. Kidder GM, Vanderhyden BC. Bidirectional communication between oocytes and follicle cells: ensuring oocyte developmental competence. Can J Physiol Pharmacol. 2010; 88:399–413. [PubMed: 20555408]
3. El-Hayek S, Clarke HJ. Control of oocyte growth and development by intercellular communication within the follicular niche. Res Probl Cell Differ. 2016; 58:191–224.
4. Wassarman PM, Litscher ES. Biogenesis of the mouse egg's extracellular coat, the zona pellucida. Curr Top Dev Biol. 2013; 102:243–266. [PubMed: 23287036]
5. Schroeder TE. Microfilament-mediated surface change in starfish oocytes in response to 1-methyladenine: implications for identifying the pathway and receptor sites for maturation-inducing hormones. J Cell Biol. 1981; 90:362–371. [PubMed: 6270153]
6. Albertini D, Combelles C, Benecchi E, Carabatsos M. Cellular basis for paracrine regulation of ovarian follicle development. Reproduction. 2001; 121:647–653. [PubMed: 11427152]
7. Makabe S, Naguro T, Stallone T. Oocyte-follicle cell interactions during ovarian follicle development, as seen by high resolution scanning and transmission electron microscopy in humans. Microsc Res Techn. 2006; 69:436–449.
8. Li R, Albertini DF. The road to maturation: somatic cell interaction and self-organization of the mammalian oocyte. Nat Rev Mol Cell Biol. 2013; 14:141–152. [PubMed: 23429793]
9. Macaulay AD, Gilbert I, Caballero J, Barreto R, Fournier E, Tossou P, Sirard MA, Clarke HJ, Khandjian EW, Richard FJ, et al. The gametic synapse: RNA transfer to the bovine oocyte. Biol Reprod. 2014; 91:90. [PubMed: 25143353]
10. Jaffe LA, Egbert JR. Regulation of mammalian oocyte meiosis by intercellular communication within the ovarian follicle. Ann Rev Physiol. 2016; 79:237–260. [PubMed: 27860834]
11. Carabatsos MJ, Sellitto C, Goodenough DA, Albertini DF. Oocyte-granulosa cell heterologous gap junctions are required for the coordination of nuclear and cytoplasmic meiotic competence. Dev Biol. 2000; 226:167–179. [PubMed: 11023678]
12. Simon A, Goodenough D, Li E, Paul D. Female infertility in mice lacking connexin 37. Nature. 1997; 385:525–529. [PubMed: 9020357]

13. Gittens JE, Barr KJ, Vanderhyden BC, Kidder GM. Interplay between paracrine signaling and gap junctional communication in ovarian follicles. J Cell Sci. 2005; 118:113–122. [PubMed: 15585573]
14. Lowther KM, Favero F, Yang CR, Taylor HS, Seli E. Embryonic poly(A)-binding protein is required at the preantral stage of mouse folliculogenesis for oocyte-somatic communication. Biol Reprod. 2017; 96:341–351. [PubMed: 28203794]
15. Matzuk M, Burns K, Viveiros M, Eppig J. Intercellular communication in the mammalian ovary: oocytes carry the conversation. Science. 2002; 296:2178–2180. [PubMed: 12077402]
16. Clarke HJ. Regulation of germ cell development by intercellular signaling in the mammalian ovarian follicle. Wiley Interdiscip Rev Dev Biol. 2018; 7:e294.
17. Albertini DF, Rider V. Patterns of intercellular connectivity in the mammalian cumulus-oocyte complex. Microsc Res Techn. 1994; 27:125–133.
18. Barrett SL, Shea LD, Woodruff TK. Noninvasive index of cryorecovery and growth potential for human follicles in vitro. Biol Reprod. 2010; 82:1180–1189. [PubMed: 20200211]
19. Svitkina TM. Ultrastructure of protrusive actin filament arrays. Curr Opin Cell Biol. 2013; 25:574–581. [PubMed: 23639311]
20. Jaiswal R, Breitsprecher D, Collins A, Correa IR Jr, Xu MQ, Goode BL. The formin Daam1 and fascin directly collaborate to promote filopodia formation. Curr Biol. 2013; 23:1373–1379. [PubMed: 23850281]
21. Vignjevic D, Kojima S, Aratyn Y, Danciu O, Svitkina T, Borisy GG. Role of fascin in filopodial protrusion. J Cell Biol. 2006; 174:863–875. [PubMed: 16966425]
22. He K, Sakai T, Tsukasaki Y, Watanabe TM, Ikebe M. Myosin X is recruited to nascent focal adhesions at the leading edge and induces multi-cycle filopodial elongation. Sci Rep. 2017; 7:13685. [PubMed: 29057977]
23. Boyd JL, Skove SL, Rouanet JP, Pilaz LJ, Bepler T, Gordan R, Wray GA, Silver DL. Human-chimpanzee differences in a FZD8 enhancer alter cell-cycle dynamics in the developing neocortex. Curr Biol. 2015; 25:772–779. [PubMed: 25702574]
24. Su YQ, Sugiura K, Eppig JJ. Mouse oocyte control of granulosa cell development and function: paracrine regulation of cumulus cell metabolism. Semin Reprod Med. 2009; 27:32–42. [PubMed: 19197803]
25. Gilchrist RB, Lane M, Thompson JG. Oocyte-secreted factors: regulators of cumulus cellfunction and oocyte quality. Hum Reprod Update. 2008; 14:159–177. [PubMed: 18175787]
26. Zhang H, Liu K. Cellular and molecular regulation of the activation of mammalian primordial follicles: somatic cells initiate follicle activation in adulthood. Hum Reprod Update. 2015; 21:779–786. [PubMed: 26231759]
27. Conti M, Hsieh M, Musa Zamah A, Oh JS. Novel signaling mechanisms in the ovary during oocyte maturation and ovulation. Mol Cell Endocrinol. 2012; 356:65–73. [PubMed: 22101318]
28. Peng J, Li Q, Wigglesworth K, Rangarajan A, Kattamuri C, Peterson RT, Eppig JJ, Thompson TB, Matzuk MM. Growth differentiation factor 9:bone morphogenetic protein 15 heterodimers are potent regulators of ovarian functions. Proc Natl Acad Sci USA. 2013; 110:E776–785. [PubMed: 23382188]
29. Dong J, Albertini DF, Nishimori K, Kumar RM, Lu N, Matzuk M. Growth differentiation factor-9 is required during early ovarian folliculogenesis. Nature. 1996; 383:531–535. [PubMed: 8849725]
30. Carabatsos MJ, Elvin J, Matzuk MM, Albertini DF. Characterization of oocyte and follicle development in growth differentiation factor-9-deficient mice. Dev Biol. 1998; 204:373–384. [PubMed: 9882477]
31. Sun J, He H, Xiong Y, Lu S, Shen J, Cheng A, Chang WC, Hou MF, Lancaster JM, Kim M, et al. Fascin protein is critical for transforming growth factor beta protein-induced invasion and filopodia formation in spindle-shaped tumor cells. J Biol Chem. 2011; 286:38865–38875. [PubMed: 21914811]
32. Buccione R, Vanderhyden BC, Caron PJ, Eppig JJ. FSH-induced expansion of the mouse cumulus oophorus in vitro is dependent upon a specific factor(s) secreted by the oocyte. Dev Biol. 1990; 138:16–25. [PubMed: 2155145]

33. Ge ZJ, Schatten H, Zhang CL, Sun QY. Oocyte ageing and epigenetics. Reproduction. 2015; 149:R103–114. [PubMed: 25391845]
34. Nagaoka SI, Hassold TJ, Hunt PA. Human aneuploidy: mechanisms and new insights into an age-old problem. Nat Rev Genet. 2012; 13:493–504. [PubMed: 22705668]
35. Titus S, Li F, Stobezki R, Akula K, Unsal E, Jeong K, Dickler M, Robson M, Moy F, Goswami S, et al. Impairment of BRCA1-related DNA double-strand break repair leads to ovarian aging in mice and humans. Sci Transl Med. 2013; 5:172ra121.
36. Fragouli E, Spath K, Alfarawati S, Kaper F, Craig A, Michel CE, Kokocinski F, Cohen J, Munne S, Wells D. Altered levels of mitochondrial DNA are associated with female age, aneuploidy, and provide an independent measure of embryonic implantation potential. PLoS Genet. 2015; 11:e1005241. [PubMed: 26039092]
37. Duncan FE, Hornick JE, Lampson MA, Schultz RM, Shea LD, Woodruff TK. Chromosome cohesion decreases in human eggs with advanced maternal age. Aging Cell. 2012; 11:1121–1124. [PubMed: 22823533]
38. Haverfield J, Nakagawa S, Love D, Tsichlaki E, Nomikos M, Lai FA, Swann K, FitzHarris G. Ca(2+) dynamics in oocytes from naturally-aged mice. Sci Rep. 2016; 6:19357. [PubMed: 26785810]
39. El-Hayek S, Clarke HJ. Follicle-stimulating hormone increases gap junctional communication between somatic and germ-line follicular compartments during murine oogenesis. Biol Reprod. 2015; 93:47. [PubMed: 26063870]
40. Jiao ZX, Xu M, Woodruff TK. Age-associated alteration of oocyte-specific gene expression in polar bodies: potential markers of oocyte competence. Fertil Steril. 2012; 98:480–486. [PubMed: 22633262]
41. Hadek R. The structure of the mammalian egg. Int Rev Cytol. 1965; 18:29–71. [PubMed: 5337036]
42. Brower PT, Schultz RM. Intercellular communication between granulosa cells and mouse oocytes: existence and possible nutritional role during oocyte growth. Dev Biol. 1982; 90:144–153. [PubMed: 7199496]
43. Da Silva-Buttkus P, Jayasooriya GS, Mora JM, Mobberley M, Ryder TA, Baithun M, Stark J, Franks S, Hardy K. Effect of cell shape and packing density on granulosa cell proliferation and formation of multiple layers during early follicle development in the ovary. J Cell Sci. 2008; 121:3890–3900. [PubMed: 19001500]
44. Zhang D, Zhang X, Zeng M, Yuan J, Liu M, Yin Y, Wu X, Keefe DL, Liu L. Increased DNA damage and repair deficiency in granulosa cells are associated with ovarian aging in rhesus monkey. J Assist Reprod Genet. 2015; 32:1069–1078. [PubMed: 25957622]
45. Molinari E, Bar H, Pyle AM, Patrizio P. Transcriptome analysis of human cumulus cells reveals hypoxia as the main determinant of follicular senescence. Mol Hum Reprod. 2016; 22:866–876. [PubMed: 27268410]
46. Ratchford AM, Esguerra CR, Moley KH. Decreased oocyte-granulosa cell gap junction communication and connexin expression in a type 1 diabetic mouse model. Mol Endocrinol. 2008; 22:2643–2654. [PubMed: 18829945]
47. O'Brien MJ, Pendola JK, Eppig JJ. A revised protocol for in vitro development of mouse oocytes from primordial follicles dramatically improves their developmental competence. Biol Reprod. 2003; 68:1682–1686. [PubMed: 12606400]
48. Eppig JJ, Wigglesworth K. Development of mouse and rat oocytes in chimeric reaggregated ovaries after interspecific exchange of somatic and germ cell components. Biol Reprod. 2000; 63:1014–1023. [PubMed: 10993822]

Highlights

- Oocyte development requires on-going communication with somatic cells of the follicle
- Communication depends on filopodia that extend from the somatic cells to the oocyte
- The oocyte induces the filopodia, by producing factors that act on the follicle cells
- Fewer filopodia couple the two cell types in aged females, impairing communication

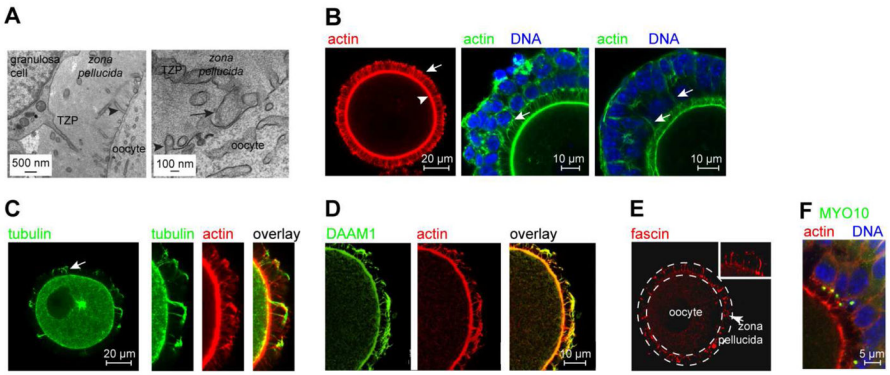

Figure 1. TZPs are specialized filopodia

(A) Left: TZP emanating from a granulosa cell. Arrowhead indicates an oocyte microvillus. Right: TZP reaching the oocyte. Arrow indicates bulbous 'foot'. (B) Left: Oocyte stained using the actin-binding dye, phalloidin. The granulosa cell bodies have been removed to improve the resolution of the TZPs (arrow), which remain embedded in the *zona pellucida*. Arrowhead indicates the oocyte cortex. Middle, Right: GOCs stained using phalloidin. Middle: Multiple TZPs extend from each granulosa cell, often apparently from a single origin (arrow). Right: Actin-rich filaments (arrows) sometimes extend from peripheral layers of granulosa cells to the oocyte. (C) Oocyte stained using anti-tubulin and phalloidin. Left: Arrow indicates tubulin-rich TZP. Right: Some tubulin-TZPs also contain actin. (D) DAAM1 is present in TZPs. (E) Fascin is present in TZPs. The *zona pellucida* is traced by the dashed lines. Inset shows higher magnification. (F) MYO10 foci are present on the apical side of granulosa cells adjacent to the *zona pellucida*. No foci are detected in peripheral layers.

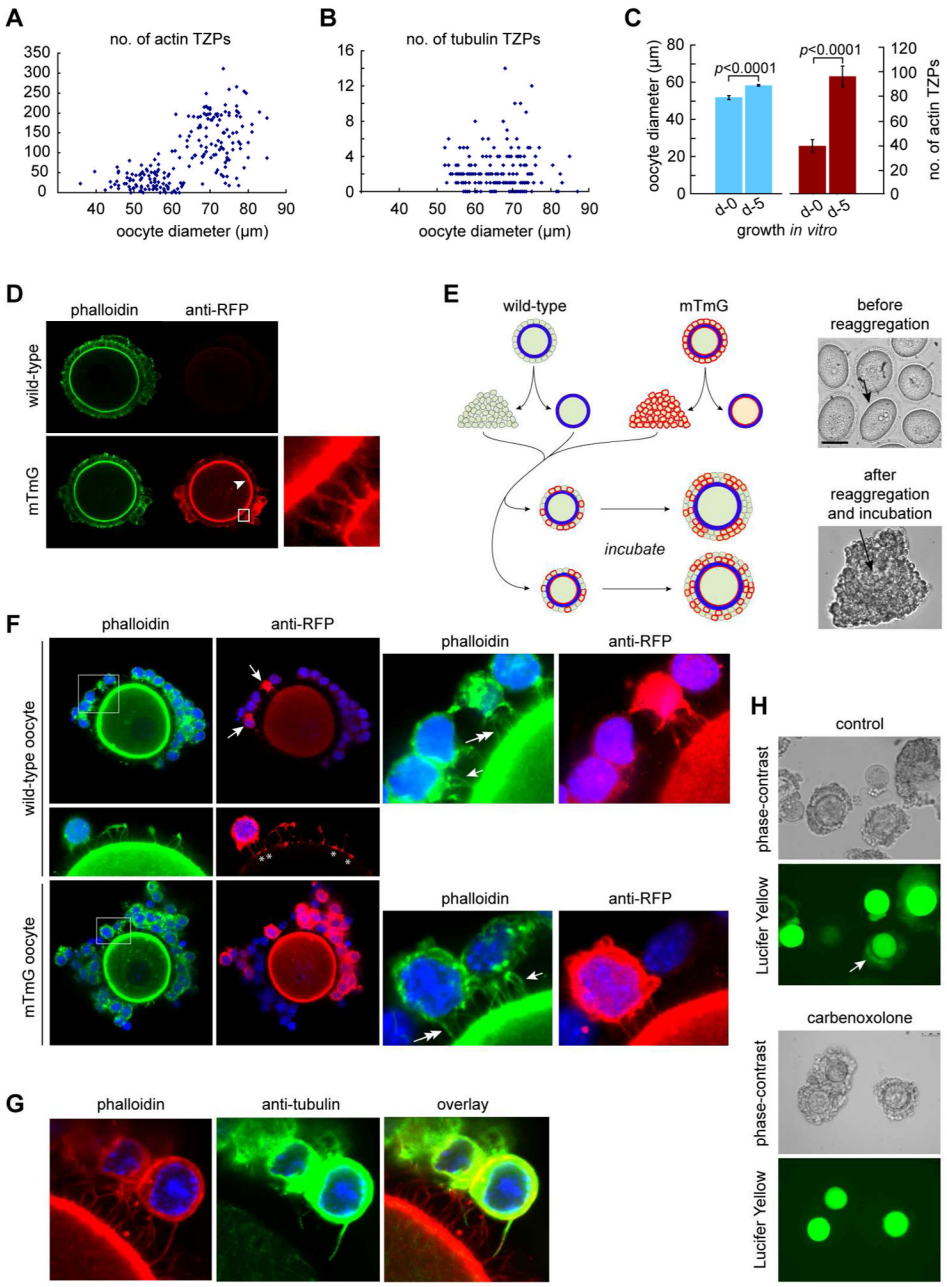

Figure 2. Granulosa cells elaborate new TZPs during oocyte growth

(A) Oocytes at different stages of growth were stained using phalloidin and the number of TZPs in an equatorial confocal optical section was counted. (B) As in (A) except that the oocytes were stained using anti-tubulin. (C) Oocyte diameter and number of actin-TZPs were determined in GOCs immediately after isolation or after 5 days of growth *in vitro*. (D) GOCs of wild-type (upper) or mTmG (lower) mice were stained using phalloidin and anti-RFP. Anti-RFP stains TZPs (inset) as well as the oocyte membrane (arrowhead) of mTmG mice. (E) Left: Reaggregation strategy. Right, upper: oocytes prior to reaggregation. Arrow indicates *zona pellucida*. Right, lower: reaggregated complex after 5 days of incubation.

Arrow indicates oocyte. (F) Reaggregated complexes after incubation. Some granulosa cells have been removed to enable TZPs to be seen more clearly. Upper: Wild-type oocyte, whose membrane is not stained by anti-RFP, enclosed by wild-type and mTmG (arrows) granulosa cells. Right panel shows enlargement of the boxed area. TZPs of wild-type granulosa cells are stained by phalloidin only (single arrow); TZPs of mTmG granulosa cells are also stained by anti-RFP (double arrow). Middle: Asterisks illustrate where TZPs of mTmG granulosa cells contact the surface of a wild-type oocyte. Lower: mTmG oocyte, whose membrane is stained by anti-RFP, enclosed by wild-type and mTmG granulosa cells. Right panel shows enlargement of the boxed area. Single arrow and double arrows indicate TZPs as above. (G) TZP stained by both phalloidin and anti-tubulin. (H) Lucifer Yellow was injected into the oocyte of reaggregated complexes. Upper: bright-field; lower: dark-field. Arrow shows fluorescence in granulosa cells. Lower paired panels show complexes incubated in the gap junction blocker, carbenoxolone. See also Figure S1.

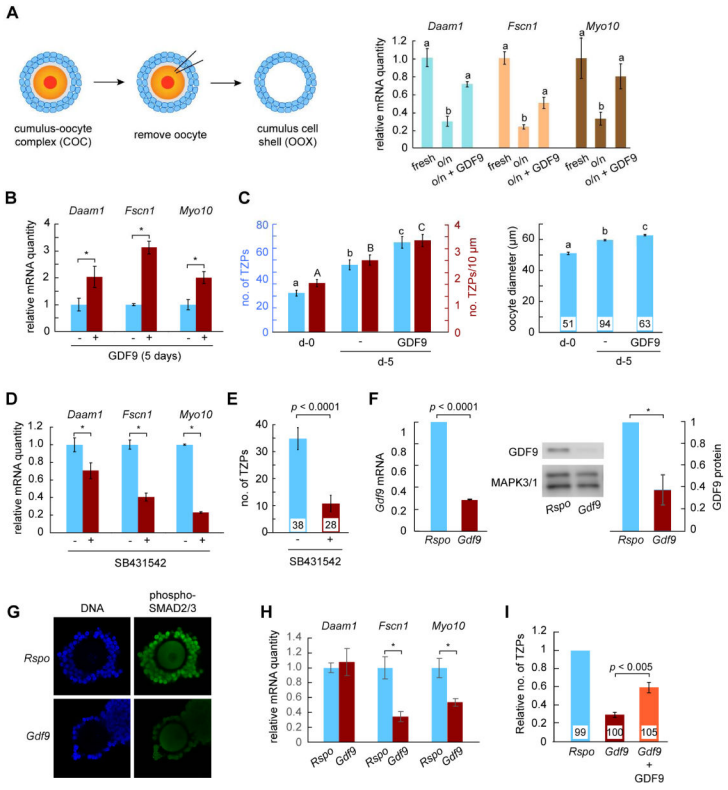

Figure 3. Oocyte-derived GDF9 promotes generation of new TZPs

(A) Left: Oocytectomy procedure. Oocytes were removed from COCs and the cumulus cell shells were harvested immediately (fresh) or cultured overnight on the absence or presence of GDF9. Right: Quantity of the indicated mRNAs, each normalized to the fresh group. (B) GOCs were incubated in the absence or presence of GDF9. The indicated mRNAs were quantified in the granulosa cells relative to *Actb*. Results normalized to culture in the absence of GDF9. (C) GOCs were collected as for (B) and either fixed immediately or incubated as shown. The number (blue bars) and density (red bars) of actin-TZPs and oocyte diameter were determined using confocal images. (D) GOCs were incubated overnight in the absence or presence of the SMAD signaling inhibitor, SB431542. mRNAs were quantified as in (A). (E) GOCs were incubated in the absence or presence of SB431542 for three days. The number of actin-TZPs was determined as in (C). (F) RNAi targeting *Rspo* (control) or *Gdf9* was injected into the oocyte of GOCs. Three days later, mRNA and protein in the oocyte were measured using quantitative RT-PCR and immunoblotting, respectively. mRNA was normalized to *Actb*; protein to MAPK3/1. A representative immunoblot is shown. (G) Following RNAi injection and incubation for two days, GOCs were stained using anti-phosphorylated SMAD2/3. (H) Following RNAi injection, GOCs were incubated for five days. mRNAs were quantified in the granulosa cells relative to *Actb*. (I) Following RNAi injection, GOCs were incubated for five days. The number of actin-TZPs was determined as in (C) and normalized to the number in the *Rspo*-injected group. For C, E and I, number of oocytes examined is shown at the base of each bar. See also Figure S2.

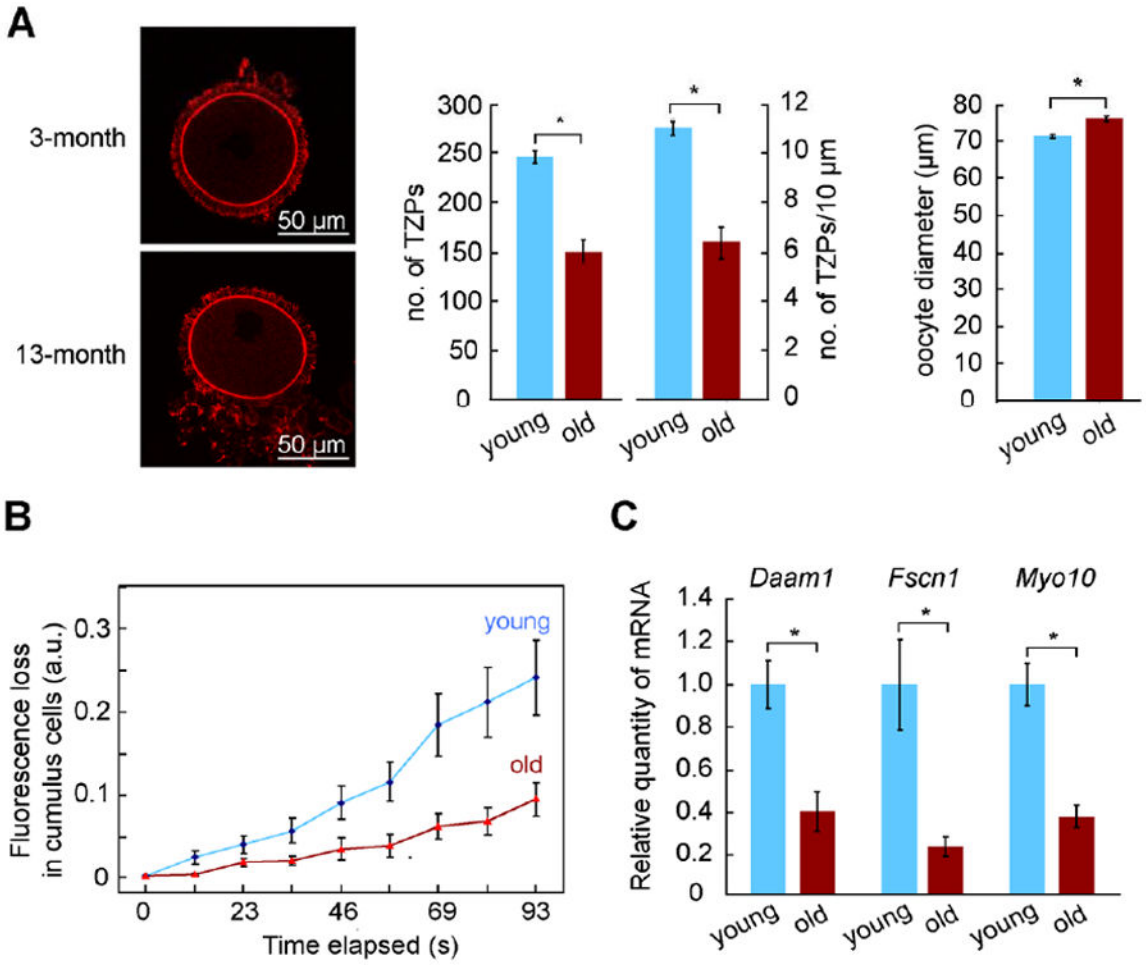

Figure 4. Aged granulosa cells have an impaired ability to generate TZPs

(A) Left: Phalloidin-stained TZPs in oocytes from 3-month and 13-month females. Right: The number and density of TZPs and oocyte diameter were determined from confocal images. (B) FLIP was performed on COCs obtained as in (A). A more rapid loss of fluorescence in the cumulus cells following bleaching of the oocyte indicates more extensive gap junctional coupling. (C) COCs were recovered from antral follicles of young (3-month) or aged (13-month) mice. The indicated mRNAs were quantified in the granulosa cells relative to *Actb*. Total number of oocytes in (A) was 32 (3-month) and 26 (13-month). See also Figure S3.

KEY RESOURCES TABLE

Reagent or resource	Source	Identifier
Antibodies		
Rabbit anti-α-actin	Abnova	H00000060-M01; RRID: AB_425284
Rabbit anti-CPEB1	Affinity Bioreagents	PA1-1100; RRID: AB_2083772
Goat anti-DAAM1	Santa Cruz	55929; RRID: AB_2089450
Mouse anti-fascin (1: 200)	Abcam	78487; RRID: AB_1566203
Goat anti-mouse GDF9 (1:1000)	R & D	AF739; RRID: AB_2111517
Rabbit anti-MAPK3/1	Cell Signaling	9102; RRID: AB_330744
Rabbit anti-Myo10 (1:200)	SDIX	2243.00.02; RRID: AB_876260
Rabbit anti-Myo10 (1:200)	Sigma	HPA024223; RRID: AB_1854248
Rabbit anti-RFP (1:400)	Cedarlane	600-401-379; RRID: AB_2209751
Rabbit anti-phospho-SMAD2/3 (1:200)	Cell Signalling	8828; RRID: AB_2631089
Rabbit anti-TACC3	Abcam	AB134154; RRID: n/a
Mouse anti-β-tubulin (1:200)	Sigma	T8203; RRID: AB_1841230
Rabbit anti-goat IgG-Alexa 546 (1:200)	Thermo Fisher	A21085; RRID: AB_2535742
Goat anti-mouse IgG-Alexa 647 (1:200)	Thermo Fisher	A21236; RRID: AB_2535805
Goat anti-rabbit IgG-Alexa 488 (1:200)	Thermo Fisher	A11008; RRID: AB_143165
Donkey anti-goat IgG-HRP (1:5000)	Promega	V8051; RRID: AB_430838
Goat anti-mouse IgG-HRP (1:5000)	Promega	W4021; RRID: AB_430834
Goat anti-rabbit IgG-HRP (1:5000)	Promega	W4011; RRID: AB_430833
Fluorescent reagents		
Calcein-AM (1 μM)	Thermo Fisher	LSC1430
FM1-43 (5 μg/ml)	Life Technologies	T35356
Lucifer Yellow (100 mM)	Thermo Fisher	L453
Phalloidin-Alexa 488 (1:100)	Thermo Fisher	A12379
Phalloidin-TRITC (1:100)	Sigma	P1951
Growth factors		
Mouse growth-differentiation factor 9 (100 ng/ml)	R & D Systems	739-G9-010
Oligonucleotides		
Actb primers: F: 5′-GGCTGTATTCCCCTCCATCG-3′; R: 5′-CCAGTTGGTAACAATGCCATGT-3′		
Daam1 primers: F: 5′-GCGGCTGCTCAGAGTATAGAAA-3′; R: 5′-AAACATGGCTTCCCTGTGTTTG -3′		
Fscn1 primers: F: 5′-AGAACGCCAGCTGCTACTTT-3′; R: 5′-CGAGGAATCACTACCCACCG -3′		
Myo10 primers: F: 5′-TCCAGACAGACTATGGGCAGG-3′; R: 5′-GGAAGCCATGTCGTCCACG -3′		
Experimental Models: Organisms/Strains		
CD-1 mice	Charles River	

Reagent or resource	Source	Identifier
mTmG mice	Jackson Laboratories	007676; RRID:IMSR_JAX:007676